



# Evaluation of biliary anatomy in the caudate lobe using drip infusion cholangiography-computed tomography

Hiromi Edo<sup>1</sup> · Ryuzo Sekiguchi<sup>1</sup> · Naoki Edo<sup>2</sup> · Akiko Kajiyama<sup>1</sup> · Masashi Nagamoto<sup>1</sup> · Tatsuya Gomi<sup>1</sup>

Published online: 17 November 2018  
© Springer Science+Business Media, LLC, part of Springer Nature 2018

## Abstract

**Purpose** This study aimed to retrospectively evaluate the caudate branches (CBs), which are bile ducts originating from the caudate lobe (CL), using drip infusion cholangiography with computed tomography (DIC-CT).

**Methods** The confluence patterns of CBs were evaluated in 185 adult patients undergoing DIC-CT. The following bile duct features were evaluated: (a) number of depicted CBs; (b) identification of the caudate portion from which the CBs were derived; (c) identification of the confluence site of a CB; and (d) whether there was a difference in the confluence site of the CBs depending on the position of the right posterior hepatic duct (RPHD) and the portal vein (PV).

**Results** DIC-CT enabled detection of a total of 640 bile ducts from the CL in 185 patients, and the total number of CBs from the Spiegel lobe (SP), the paracaval portion, and the caudate process (CP) were 347 (54.2%), 112 (17.5%), and 181 (28.2%), respectively. In the SP, over 60% of CBs joined the left hepatic duct system (LHDS). The positional relationship between the RPHD and the PV was divided into a supra-portal course ( $n = 168$ ) and an infra-portal course ( $n = 17$ ). The number of CBs joining the LHDS was significantly different between a supra-portal course and an infra-portal course ( $p = 0.0484$ ).

**Conclusion** CBs were depicted by DIC-CT in 98.9% of the subjects, and a detailed evaluation was possible. The number of CBs joining the LHDS was associated with the position of the RPHD and the PV.

**Keywords** DIC-CT · Bile ducts · Liver · Caudate lobe

## Introduction

In recent years, the techniques for hepatic surgery have progressed; however, the surgical operations that include the caudate lobe (CL) are still challenging due to its deep location within the liver and its proximity to hepatic hilar structures [1–4]. Knowledge of anatomical variations of the biliary system helps reduce postoperative complications, which include injury to contralateral biliary ducts and bile leakage.

Previous reports have described the dissection of bile ducts and the position of the portal vein and biliary ducts

with respect to each other [5, 6], but they do not include caudate branches (CBs). Detailed analysis concerning the CBs has been exclusively performed using liver casts and drip infusion cholangiography with computed tomography (DIC-CT) [7–10]. As the CBs are considerably thin, the depiction of CBs in magnetic resonance cholangiopancreatography (MRCP) and gadolinium-ethoxybenzyl-diethylenetriamine pentaacetic acid (Gd-EOB-DTPA)-enhanced magnetic resonance imaging (MRI) is difficult. On the contrary, DIC-CT can depict thin bile ducts, such as CBs [11, 12].

However, DIC-CT is becoming less common because the intravenous cholangiographic contrast media is available in only a few countries [5]. Thus, the analysis of CB using DIC-CT is limited. To the best of our knowledge, only two reports have evaluated the details of CBs using DIC-CT [8, 9].

The purpose of this study was to identify the number of CBs that could be depicted by DIC-CT to evaluate the

✉ Hiromi Edo  
hiromi.edo@med.toho-u.ac.jp

<sup>1</sup> Department of Radiology, Toho University Ohashi Medical Center, 2-22-36 Ohashi Meguroku, Tokyo, Japan

<sup>2</sup> Department of Internal Medicine, Teikyo University School of Medicine, Tokyo, Japan

features of CBs, and to examine whether the confluence sites of CBs were dependent on the course of the portal vein.

## Materials and methods

### Ethical considerations

This study complied with the ethical guidelines of the Declaration of Helsinki, and was approved by the institutional ethics committee (H16082). Written informed consent for participation was not required from the patients as the study was retrospective and patient records were anonymously analyzed.

### Patients

In total, 197 consecutive adult patients underwent DIC-CT at our medical center between July 2013 and November 2014. Twelve cases were excluded due to poor depiction of an entire biliary tree, history of a hepatectomy, or hepaticojejunostomy. Finally, 185 patients (85 males, 100 females; mean age 58 years, range 25–90 years) were evaluated. The reasons for undergoing DIC-CT in this study were cholelithiasis (124 patients), acute cholecystitis (29 patients), gallbladder polyps (15 patients), common bile duct stones (11 patients), bile leakage (three patients), bile duct stenosis (two patients), and gallbladder cancer (one patient). Patients were divided into two groups based on two patterns depicting the positional relationship between the right posterior bile duct (RPBD) and the portal vein (PV): a supra-portal course or an infra-portal course.

### DIC-CT examinations

A multi-detector row helical CT scanner (Aquilion; Toshiba, Tokyo, Japan) was used. Sixty-four-detector row CT scans were obtained with the following parameters: 1 mm collimation, a beam pitch of 0.844, and a tube current of 120 kV with Auto MA. Transverse sections were reconstructed with 1-mm-thick sections at 0.5-mm intervals. The reconstruction field of view was set to the area around the liver to improve spatial resolution. A biliary contrast agent, consisting of 100 mL of meglumine iotroxate (50 mg/mL Biliscopin; Schering, Berlin, Germany), was administered for 30 min, 1 h before scanning. A paging method was used, in which 1–2-mm slice transverse CT images were observed by scrolling. In addition, multiplanar reconstruction images, maximum intensity projection (MIP), and volume rendering (VR) were also used supplementarily.

## Analysis of DIC-CT images

We evaluated the following bile duct features: (a) the number of depicted CBs; (b) identification of the caudate portion from which the CBs were derived; (c) identification the confluence site of a CB; and (d) whether there was a difference in the confluence site of the CBs depending on the course of the portal vein (a supra-portal course or an infra-portal course). When some branches formed a common canal, each branch was counted. The CL is divided into three portions: the Spiegel lobe (SP), the paracaval portion (PC), and the caudate process (CP), according to Kumon [7, 10] (Fig. 1). A supra-portal course refers to a pattern in which the RPHD runs on the cranial side of the PV; it is the common form. On the other hand, an infra-portal course refers to a pattern in which a part of the RPHD runs on the caudal side of the PV, as previously reported [6].

The LHDS included B2, the left lateral segmental ducts (B2 + 3), and the left hepatic duct. The middle hepatic duct system (MHDS) included the common hepatic duct and trifurcation types. The right hepatic duct system (RHDS) included the right hepatic duct, the right anterior hepatic duct, the right posterior hepatic duct, B5, B6, and B8.

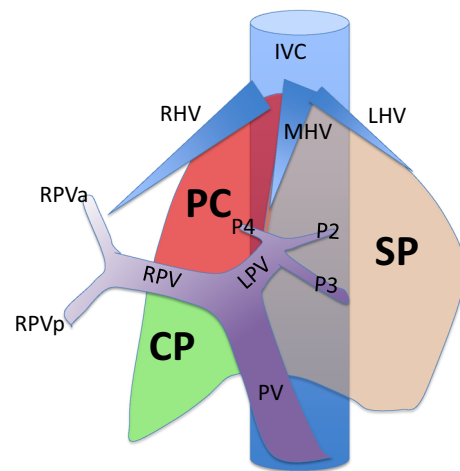


**Fig. 1** Schematic diagrams of the frontal projection. The Spiegel lobe (SP) is the area to the left of the inferior vena cava (IVC) and ligamentum venosum (orange areas). The paracaval portion (PC) is in front of the IVC, and between the middle hepatic vein (MHV) and the right hepatic vein (RHV), and lies cranial to the portal bifurcation (red areas). The caudate process is in front of the IVC, caudal to the portal bifurcation, and dorsal to the right portal pedicle (green areas). *SP* Spiegel lobe, *PC* paracaval portion, *CP* caudate process, *IVC* inferior vena cava, *PV* main portal vein, *RPV* right portal vein, *LPV* left portal vein, *RPVa* right anterior segmental portal vein, *RPVp* right posterior segmental portal vein, *P2* portal vein for hepatic segment II, *P3* portal vein for hepatic segment III, *P4* portal vein for hepatic segment IV [22]

## Statistical analysis

Comparisons between groups were performed using the Mann–Whitney *U* test for continuous variables.  $P < 0.05$  was considered statistically significant. All statistical analyses were performed with EZR (Saitama Medical Center, Jichi Medical University, Saitama, Japan), which is a graphical user interface for R (The R Foundation for Statistical Computing, Vienna, Austria).

## Results

### Number of depicted CBs

DIC-CT enabled detection of a total of 640 bile ducts from the CL in 98.9% (183/185) of cases. Figure 2 demonstrates typical images of CBs on the DIC-CT. Zero to nine CBs, with a mean of 3.45, were detected per liver in 185 patients (Table 1).

### Identification of caudate portion from which the CBs were derived

The total number of CBs from the SP, PC, and CP were 347 (54.2%), 112 (17.5%), and 181 (28.2%), respectively (Table 1).

### Identification of the confluence site of the CB

We identified CBs joined to the RHDS ( $n = 341$ ), MHDS ( $n = 16$ ), and LHDS ( $n = 283$ ). The confluence sites of the bile ducts from each portion of the CL are shown in Table 2. Table 3 shows the percentage of confluence sites of CBs from each liver portion; half of the CBs joined the RHDS, and the other half of the CBs joined the LHDS. In the CP, over 90% of CBs joined the RHDS. In the SP, over 60% of CBs joined the LHDS.

### Difference in the confluence site of the CBs depending on the course of the portal vein (supra-portal or infra-portal course)

The positional relationship between the RPHD and the PV was divided into two types: a supra-portal course ( $n = 168$ ) and an infra-portal course ( $n = 17$ ). Figures 3 and 4 demonstrate the typical images of a supra-portal course and an infra-portal course, respectively.

The number of CBs joining the LHDS was significantly different between a supra-portal course and an infra-portal course ( $p = 0.0484$ ) (Table 4, Fig. 5). Compared with the supra-portal course, an infra-portal course had more CBs, which drained into LHDS. The number of CBs joining the RHDS was mildly different between a supra-portal course and an infra-portal course ( $p = 0.0802$ ) (Table 4, Fig. 5).

**Fig. 2** A 66-year-old woman with five CBs (arrows) detected using drip infusion cholangiography with computed tomography. Slab-MIP with 20 mm thickness (**a**, **b** coronal view, **c** transverse view) and MIP in the anterior right view (**d**) depicts five CBs. Four CBs join into the RHD and one CB joins into the LHD. One CB (yellow arrow) is derived from the paracaval portion, one CB (green arrow) is derived from the caudate process, and three CBs (black arrows) are derived from the Spiegel lobe. MIP maximum intensity projection, CB caudate branch, RHD right hepatic duct, LHD left hepatic duct

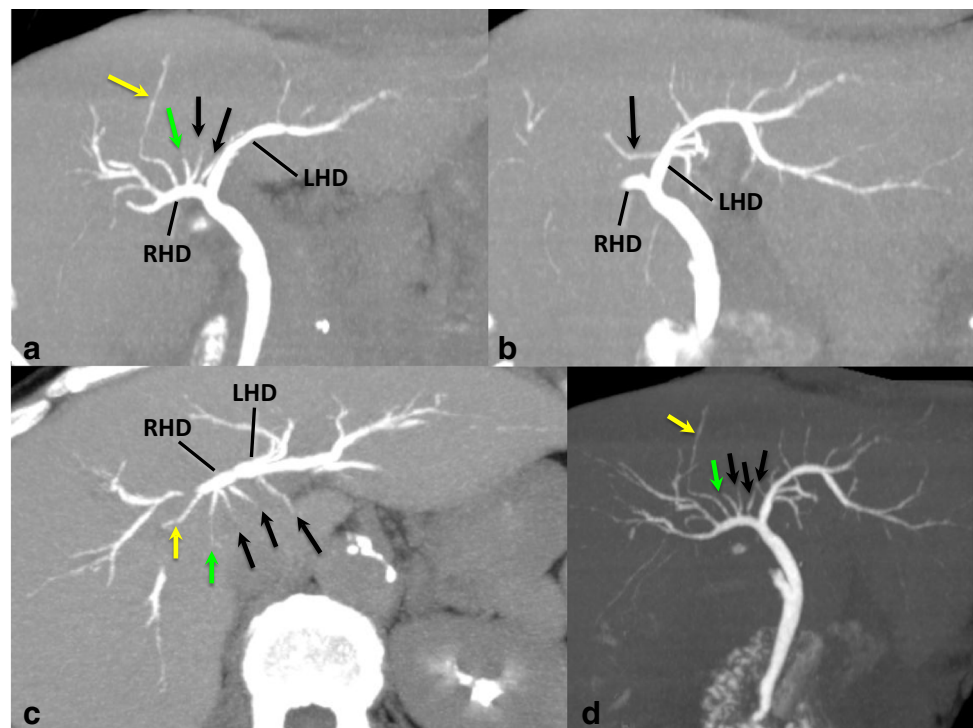


**Table 1** Number of depicted bile ducts from the caudate lobe and each portion

Number	Spiegel lobe	Paracaval portion	Caudate process	Caudate lobe
0	13	81	31	2
1	46	96	128	12
2	83	8	25	27
3	39	0	1	56
4	3	0	0	48
5	0	0	0	30
6	1	0	0	8
7	0	0	0	1
8	0	0	0	0
9	0	0	0	1
Total	347	112	181	640
Mean (/185 patients)	1.87	0.6	0.97	3.45

**Table 2** The confluence site of the bile duct from the caudate lobe

Confluence site	Spiegel lobe	Paracaval portion	Caudate process	Total
LHDS				
B2	24	0	0	24
B2+3	21	2	0	23
LHD	180	44	12	236
MHDS				
CHD	12	0	1	13
Tri	3	0	0	3
RHDS				
RHD	57	26	25	108
RAHD	3	0	2	5
RPHD	45	38	98	181
B5	0	0	3	3
B6	2	0	40	42
B8	0	2	0	2
Total	347	112	181	640

*B2* bile ducts from segment 2, *B2+3* proximal to the fusion point of *B2* and the bile duct of segment 3, *LHD* left hepatic duct, *CHD* common hepatic duct, *Tri* trifurcation, *RHD* right hepatic duct, *RAHD* right anterior hepatic duct, *RPHD* right posterior hepatic duct, *B5* bile duct from segment 5, *B6* bile duct from segment 6, *B8* bile duct from segment 8

The infra-portal course had less CBs that drained into RHDS than did the supra-portal course. The number of CBs was similar between the supra-portal and infra-portal courses ( $p = 0.533$ ).

**Table 3** Percentage of confluence sites of CBs from each liver portion

Confluence site	Spiegel lobe	Paracaval portion	Caudate process	Caudate lobe
LHDS	225 (64.8%)	46 (41.0%)	12 (6.6%)	283 (44.2%)
MHDS	15 (4.3%)	0	1 (0.5%)	16 (2.5%)
RHDS	107 (30.8%)	66 (58.9%)	168 (92.8%)	341 (53.2%)
Total	347	112	181	640

*LHDS* left hepatic duct system, *MHDS* middle hepatic duct system, *RHDS* right hepatic duct system

### Discussion

In the current study, we have demonstrated that DIC-CT enabled visualization of one or more CBs in 98.9% of cases, and that more than half of the CBs were derived from the SP. In the entire CL and in the PC, almost equal numbers of CBs drained into RHDS and LHDS. In the SP, about 30% CBs drained into RHDS; in the CP, over 90% of CBs drained into the RHDS. The number of CBs that joined into the LHDS was greater with the infra-portal course than with the supra-portal course.

With the development of recent image technology, the biliary tree can be depicted with minimal invasion using DIC-CT, MRCP, and Gd-EOB-DTPA MRI [5]. As noted in previous reports, DIC-CT could demonstrate not only the second-order branches of the bile ducts, but also the third-order branches [11], and it provided high-resolution three-dimensional anatomical representation of very small bile ducts. In recent studies, 3D balanced turbo-field-echo sequence could depict the bile ducts and portal veins as well as DIC-CT [13]. However, even now DIC-CT was superior to conventional MRCP in the detection of the small non-expanded bile ducts such as CBs or an accessory hepatic duct [5, 14–16]. Therefore, DIC-CT is frequently used for preoperative examination of the biliary tract, prior to laparoscopic cholecystectomy and liver transplantation, due to its high-quality imaging output; this is the case despite radiation exposure and the possibility of developing adverse reactions from the infusion of meglumine iotroxate [8, 17–19].

In this study, DIC-CT could depict the CBs in 98.9% of our subjects, and the mean number of CBs detected using DIC-CT was 3.45 CBs per liver. The CB detection rate with DIC-CT in previous reports was 77% to 100%, and the mean number of CBs detected with DIC-CT was 1.86–2.68 branches per liver [8, 9]. The detection capability and detection number of CBs in this study were almost equally high or slightly higher than those of previous reports. One reason why the visualization number of CBs was slightly higher than that reported in the literature

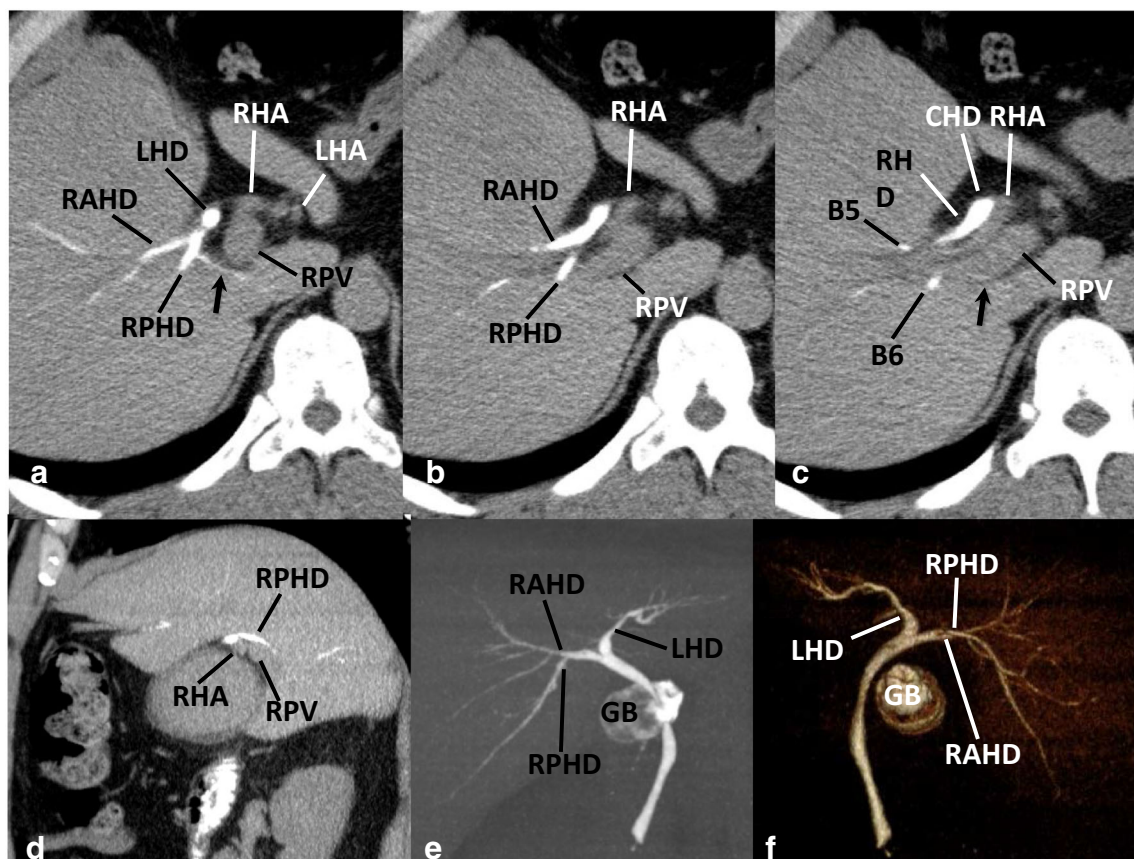


**Fig. 3** A 46-year-old man with a right posterior bile duct following a supra-portal course, as detected using drip infusion cholangiography with computed tomography. Transverse images arranged in **a** cranial to **c** caudal order, **d** the sagittal multiplanar image of reconstruction, **e** maximum intensity projection (MIP) in the anterior view, and **f** the volume-rendered (VR) image in the left posterior view are demonstrated. These images (**a–d**) show that the RPHD runs on the cranial side of the RPV. MIP and VR images show that

RAHD and RPHD form a common canal as the RHD. The black arrows point to the caudate branches; one is derived from the paracaval portion (**a**), and the other is derived from the caudate process (**c**). RAHD right anterior hepatic duct, RPHD right posterior hepatic duct, LHD left hepatic duct, RHA right hepatic artery, LHA left hepatic artery, RPV right portal vein, B5 bile duct from segment 5, B6 bile duct from segment 6, CHD common hepatic duct, LHD left hepatic duct, GB gallbladder

was thought to be related to the detailed observation (owing to thin slices) performed using the paging method.

More than half of the CBs were derived from the SP. The results of this study were similar to those of Kitami et al., in that they reported that 53.7% of the CBs were derived from SP [9]. However, Kitami et al. divided the CL into two portions, SP and PC; this differs from the present study and many other reports. In contrast, this rate was 37.8% in the report by Takamatsu et al. [8], and it was conceivable that differences in counting methods could influence the number of bile ducts identified. When the CBs formed a common canal, Takamatsu et al. counted each bile duct when the CBs originated from different portions, and they were counted as one when the CBs originated from the same area. In this study, each CB was counted regardless if they formed a common canal.

In our study, over 30% of the CBs that were derived from the SP joined into the RHDS. The percentage of CBs

that were derived from the PC and joined into the RHDS and LHDS were 58% and 41%, respectively; over 90% of the CBs that were derived from the CP joined into the RHDS. According to two reports on DIC-CT [8, 9], the frequencies of CBs from the SP that joined into the RHDS widely ranged between 10.4% and 30.1%. The frequencies of CBs from the PC that joined into the RHDS and the LHDS were 63–64% and 32–34%, respectively, and the frequencies of CBs joined into the RHDS were 93% in the CP. The results of the present study were similar to those of previous studies. Additionally, our results are similar to those of other previous reports, which analyzed CBs using percutaneous transhepatic CT cholangiography and corrosion liver casts [7, 10, 20] and, respectively, found that 35.5% and 29.2% of CBs from the SP joined into the RHDS. Percutaneous transhepatic CT cholangiography revealed that 41.2% and 58.7% of CBs from the PC joined

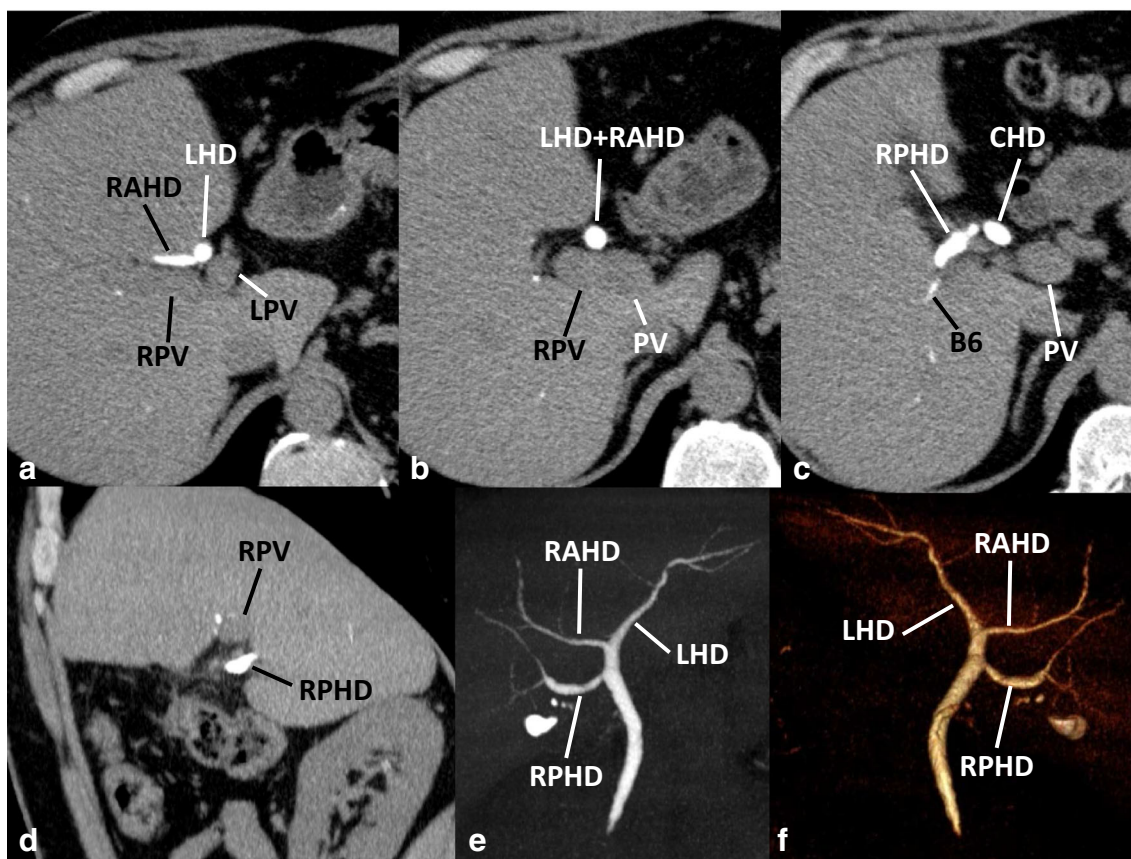


**Fig. 4** A 41-year-old man with a right posterior bile duct following an infra-portal course, as detected using drip infusion cholangiography with computed tomography. Transverse images arranged in **a** cranial to **c** caudal order, **d** the sagittal multiplanar image of reconstruction, **e** maximum intensity projection (MIP) in the anterior view, and **f** the volume-rendered (VR) image in the posterior view are demonstrated. These images (**a–d**) show that the RPHD runs on the caudal side of

the RPV, and MIP and VR images show RAHD and RPHD join into the LHD, respectively, without forming the RHD. RAHD the right anterior hepatic duct, RPV the right portal vein, LHD the left hepatic duct, LPV the left portal vein, proximal to the fusion point of LHD and RAHD, PV the main portal vein, B6 the bile duct from segment 6, CHD the common hepatic duct

**Table 4** Comparison of the number of each confluence site between both groups

	A supra-portal course	An infra-portal course	<i>p</i>
<i>n</i>	168	17	
Number of CBs joining each area			
LHDS	1 (0-5)	2 (0-5)	0.0484
MHDS	0 (0-0)	1 (0-1)	0.446
RHDS	2 (0-5)	1 (0-4)	0.0802
			Mann–Whitney <i>U</i> test

LHDS left hepatic duct system, MHDS middle hepatic duct system, RHDS right hepatic duct system

into the RHDS and LHDS, respectively, and 100% of CBs joined into the RHDS in the CP.

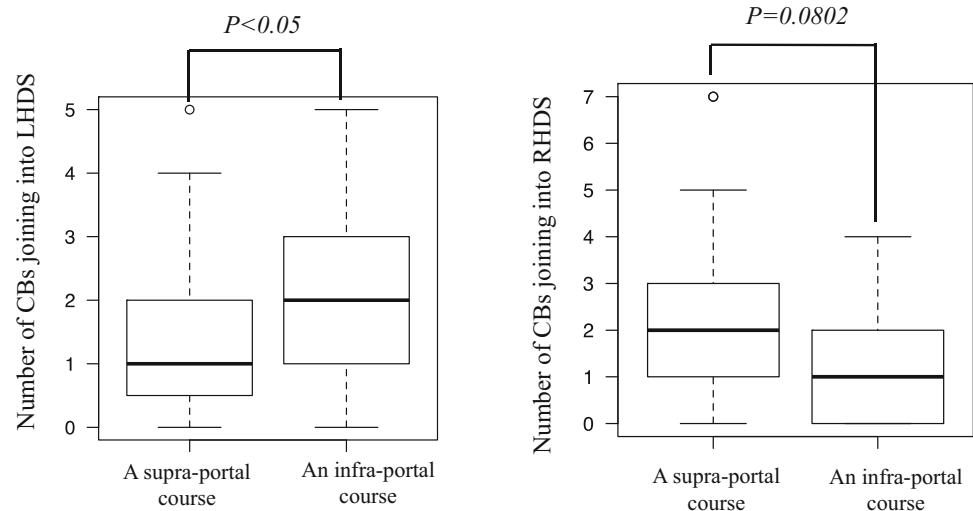
The number of CBs that joined into the LHDS was greater with the infra-portal course than with the supra-

portal course. There are currently no reports on the relationship between CB and running pattern of RPHD. Kitami et al. [6] evaluated the relative position between the bile ducts and the portal vein in their study on anatomical characteristics of bile ducts, which did not include CBs. The findings from this study demonstrate the tendency of the confluence site of CBs to differ depending on the course of RPHD, which is important anatomical knowledge for safe surgical operation of the CL.

However, this study had some limitations. First, it was a retrospective and single-center study. Therefore, in the selection of patients, the possibility of unwilling selection bias could not be amply excluded. Second, the confluence pattern of CBs was not confirmed at dissection or surgery. However, DIC-CT was superior to other imaging modalities, such as MRCP, in the detection of small non-expanded bile ducts [5, 11, 14].

In our study, DIC-CT was performed by administering meglumine iotroxate, which is a relatively safer

**Fig. 5** Comparison of the number of CBs joining into LHDS and RHDS between both groups. *CBs* caudate branches, *LHDS* left hepatic duct system, *RHDS* right hepatic duct system



intravenous biliary contrast medium than that used before [21]. Although the meglumine iotroxate agent is not available in some countries, it is widely used in the European and Asian countries. DIC-CT has some disadvantages in that it cannot aid in visualizing the bile duct without using intravenous biliary contrast medium, and there is radiation exposure. However, accurate prediction of CB anatomy is important to reduce postoperative biliary complications. Therefore, DIC-CT provides an essential improvement due to its ability to depict tiny bile ducts such as CBs [22, 23]. The technological innovation of CT imaging has been progressing, and future improvement of image quality and reduction of radiation exposure are expected to be achieved through low-tube-voltage CT, full interactive construction, and ultrahigh-resolution CT.

In conclusion, our results confirmed that DIC-CT was effective in visualizing small non-expanded bile ducts such as CBs. This study revealed that the confluence site of CBs from the SP was the RHDS in about 30% of the CBs, and it was much more frequent than had been previously reported. Other findings of CBs were similar to those in previous reports. A novel finding of this study was that the number of CBs that joined into the LHDS was greater in the group with an infra-portal course than in the group with a supra-portal course. These findings provide further insight into the anatomical variations of the biliary system, which may help reduce surgical complications in the CL.

**Acknowledgements** We would like to thank Editage ([www.editage.jp](http://www.editage.jp)) for English language editing.

**Funding** None.

### Compliance with ethical standards

**Conflicts of interest** The authors declare that they have no conflict of interest.

### References

1. Yamamoto T, Kubo S, Shuto T, Ichikawa T, Ogawa M, Hai S, Sakabe K, Tanaka S, Uenishi T, Ikebe T, Tanaka H, Kaneda K, Hirohashi K (2004) Surgical strategy for hepatocellular carcinoma originating in the caudate lobe. *Surgery* 135:595–603. <https://doi.org/10.1016/j.surg.2003.10.015>
2. Chaib E, Ribeiro MAF Jr., Silva Fde S, Saad WA, Ceconello I (2007) Surgical approach for hepatic caudate lobectomy: Review of 401 cases. *J Am Coll Surg* 204:118–127. <https://doi.org/10.1016/j.jamcollsurg.2006.09.020>
3. Wen ZQ, Yan YQ, Yang JM, Wu MC (2008) Precautions in caudate lobe resection: report of 11 cases. *World J Gastroenterol* 14:2767–2770
4. Jin Y, Wang L, Yu YQ, Zhou DE, Liu DR, Yang JJ, Peng SY, Li JT (2017) Anatomic isolated caudate lobectomy: Is it possible to establish a standard surgical flow? *World J Gastroenterol* 23:7433–7439. <https://doi.org/10.3748/wjg.v23.i41.7433>
5. Hyodo T, Kumano S, Kushihata F, Okada M, Hirata M, Tsuda T, Takada Y, Mochizuki T, Murakami T (2012) CT and MR cholangiography: advantages and pitfalls in perioperative evaluation of biliary tree. *Br J Radiol* 85:887–896. <https://doi.org/10.1259/bjr/21209407>
6. Kitami M, Takase K, Murakami G, Ko S, Tsuboi M, Saito H, Higano S, Nakajima Y, Takahashi S (2006) Types and frequencies of biliary tract variations associated with a major portal venous anomaly: analysis with multi-detector row CT cholangiography. *Radiology* 238:156–166. <https://doi.org/10.1148/radiol.2381041783>
7. Kumon M (2017) Anatomical study of the caudate lobe with special reference to portal venous and biliary branches using corrosion liver casts and clinical application. *Liver Cancer* 6:161–170. <https://doi.org/10.1159/000454682>
8. Takamatsu S, Goseki N, Nakajima K, Teramoto K, Iwai T, Arai S (2004) Distributing pattern of the bile duct of the caudate lobe on computed tomography with drip infusion cholangiography and its surgical significance. *Hepatogastroenterology* 51:29–32
9. Kitami M, Murakami G, Ko S, Takase K, Tsuboi M, Saito H, Nakajima Y, Takahashi S (2004) Spiegel's lobe bile ducts often drain into the right hepatic duct or its branches: study using drip-infusion cholangiography-computed tomography in 179 consecutive patients. *World J Surg* 28:1001–1006. <https://doi.org/10.1007/s00268-004-7483-4>

10. Kumon M (1985) [Anatomy of the caudate lobe with special reference to portal vein and bile duct]. *Acta Hepatol Jpn* 26:1193–1199 (in Japanese with English summary)
11. Yeh BM, Breiman RS, Taouli B, Qayyum A, Roberts JP, Coakley FV (2004) Biliary tract depiction in living potential liver donors: comparison of conventional MR, mangafodipir trisodium-enhanced excretory MR, and multi-detector row CT cholangiography—initial experience. *Radiology* 230:645–651. <https://doi.org/10.1148/radiol.2303021775>
12. Chen JS, Yeh BM, Wang ZJ, Roberts JP, Breiman RS, Qayyum A, Coakley FV (2005) Concordance of second-order portal venous and biliary tract anatomies on MDCT angiography and MDCT cholangiography. *AJR Am J Roentgenol* 184:70–74. <https://doi.org/10.2214/ajr.184.1.01840070>
13. Ogawa M, Ozawa Y, Ohta K, Sekiguchi T, Omata S, Urano M, Matsuo Y, Shibamoto Y (2017) Usefulness of 3D balanced turbofield-echo MR sequence evaluating the branching pattern of the intrahepatic bile ducts: comparison with drip infusion CT cholangiography. *Abdom Radiol (NY)* 42:1888–1895. <https://doi.org/10.1007/s00261-017-1093-8>
14. Saad WE, Ginat D (2008) Computed tomography and magnetic resonance cholangiography. *Tech Vasc Interv Radiol* 11:74–89. <https://doi.org/10.1053/j.tvir.2008.07.002>
15. Hirao K, Miyazaki A, Fujimoto T, Isomoto I, Hayashi K (2000) Evaluation of aberrant bile ducts before laparoscopic cholecystectomy: helical CT cholangiography versus MR cholangiography. *AJR Am J Roentgenol* 175:713–720. <https://doi.org/10.2214/ajr.175.3.1750713>
16. Ishii H, Noguchi A, Fukami T, Sugimoto R, Tada H, Takeshita H, Umehara S, Izumi H, Tani N, Yamaguchi M, Yamane T (2017) Preoperative evaluation of accessory hepatic ducts by drip infusion cholangiography with CT. *BMC Surg* 17:52. <https://doi.org/10.1186/s12893-017-0251-9>
17. Nilsson U (1987) Adverse reactions to iotroxate at intravenous cholangiography. A prospective clinical investigation and review of the literature. *Acta Radiol* 28:571–575
18. Persson A, Dahlstrom N, Smedby O, Brismar TB (2006) Three-dimensional drip infusion CT cholangiography in patients with suspected obstructive biliary disease: a retrospective analysis of feasibility and adverse reaction to contrast material. *BMC Med Imaging* 6:1. <https://doi.org/10.1186/1471-2342-6-1>
19. Fulcher AS (2004) CT cholangiography: advantages and disadvantages compared with MR cholangiography in the evaluation of the biliary tract following liver transplantation. *Liver Transpl* 10:1071–1072. <https://doi.org/10.1002/lt.20207>
20. Shinohara Y (1995) [Demonstration of caudate lobe bile ducts using 3D-CT cholangiography]. *Nihon Geka Gakkai zasshi* 96:88–96 (in Japanese with English summary)
21. Taenzler V, Volkhardt V (1979) Double blind comparison of meglumine iotroxate (Biliscopin), meglumine iodoxamate (Endobil), and meglumine ioglycamate (Biligram). *AJR Am J Roentgenol* 132:55–58. <https://doi.org/10.2214/ajr.132.1.55>
22. Edo H, Sekiguchi R, Kajiyama A, Iwasaki M, Hasegawa M, Tsunoo M, Nagamoto M, Gomi T (2017) Variations of Biliary Anatomy from the caudate Lobe by CT Cholangiography – How far can we evaluate? *ECR2017-EPOS*. <https://doi.org/10.1594/ecr2017/c-0480>.
23. Edo H, Sekiguchi R, Kajiyama A, Murata N, Nagamoto M, Gomi T (2018) Confluence patterns of bile ducts from the caudate lobe and variations in the right and left hepatic ducts: an analysis using multi-detector row computed tomography cholangiography. *ECR2018-EPOS*. <https://doi.org/10.1594/ecr2018/c-1765>.